

# A combined experimental and finite element approach to analyse the fretting mechanism of the head–stem taper junction in total hip replacement

Thom Bitter<sup>1</sup>, Imran Khan<sup>2</sup>, Tim Marriott<sup>2</sup>, Elaine Lovelady<sup>2</sup>, Nico Verdonschot<sup>1,3</sup> and Dennis Janssen<sup>1</sup>

Proc IMechE Part H:

*J Engineering in Medicine*

2017, Vol. 231 (9) 862–870

© IMechE 2017



Reprints and permissions:

sagepub.co.uk/journalsPermissions.nav

DOI: 10.1177/0954411917713774

journals.sagepub.com/home/pih



## Abstract

Fretting corrosion at the taper interface of modular hip implants has been implicated as a possible cause of implant failure. This study was set up to gain more insight in the taper mechanics that lead to fretting corrosion. The objectives of this study therefore were (1) to select experimental loading conditions to reproduce clinically relevant fretting corrosion features observed in retrieved components, (2) to develop a finite element model consistent with the fretting experiments and (3) to apply more complicated loading conditions of activities of daily living to the finite element model to study the taper mechanics. The experiments showed similar wear patterns on the taper surface as observed in retrievals. The finite element wear score based on Archard's law did not correlate well with the amount of material loss measured in the experiments. However, similar patterns were observed between the simulated micromotions and the experimental wear measurements. Although the finite element model could not be validated, the loading conditions based on activities of daily living demonstrate the importance of assembly load on the wear potential. These findings suggest that finite element models that do not incorporate geometry updates to account for wear loss may not be appropriate to predict wear volumes of taper connections.

## Keywords

Fretting, finite element modelling, total hip arthroplasty, taper junction, wear testing, wear modelling

Date received: 22 November 2016; accepted: 12 May 2017

## Introduction

A modular taper junction is often used to connect the femoral head and stem during total hip arthroplasty (THA) as it can offer the surgeon increased intra-operative flexibility that is required to restore patient anatomy. The use of a modular head allows for the adjustment of offset, which can compensate for differences in soft tissue tensioning and leg length discrepancies, thereby improving the function of the reconstructed joint. However, as early as the 1990s, corrosion has been reported as a potential disadvantage associated with the use of modular components.<sup>1,2</sup> Recent reports have observed fretting or mechanically assisted crevice corrosion in some modular junctions. This particularly appeared when using femoral heads with large diameters,<sup>3,4</sup> which in some cases caused early failure of the reconstruction.<sup>5,6</sup>

Biomechanical research into the origin of fretting corrosion at modular taper junctions has focused on

experimental testing, to investigate the fretting process, and computational modelling, investigating the effect of patient- and surgery-related variations on fretting potential. Ideally, these two methodologies should be combined, as it enables validation of computational models, but it also provides more flexibility in biomechanical testing. In this work, an attempt was made to develop a combined mechanical approach to investigate fretting corrosion. For this purpose, a novel mechanical testing setup is presented, which was mimicked in silico. This validated simulation was then used to further

<sup>1</sup>Orthopaedic Research Lab, Radboudumc, Nijmegen, The Netherlands

<sup>2</sup>Zimmer Biomet, Swindon, UK

<sup>3</sup>University of Twente, Enschede, The Netherlands

### Corresponding author:

Thom Bitter, Orthopaedic Research Lab (547), Radboudumc, P.O.Box 9101, 6500 HB, Nijmegen, The Netherlands.

Email: thom.bitter@radboudumc.nl

investigate how variations in implant assembly load and patient activity can affect the fretting wear process at the taper junction, as these cannot be easily reproduced testing in vitro.

Several experimental studies have investigated the underlying mechanical and electrochemical processes at the taper junction interface in order to further understand their contribution to fretting, ranging from simple pin-on-disc tests to in vitro tests using full implant systems.<sup>7–12</sup> Pin-on-disc tests are used to measure the fretting potential for different material combinations, while in vitro experiments are more representative of the clinical situation. In ISO 7206-6:2013 tests, the endurance and fatigue properties of THA systems can be evaluated, but these are unable to produce wear and corrosion patterns that have been observed on clinical retrievals. The first objective of this study was therefore to adapt the loading conditions in an attempt to better reproduce clinically relevant fretting corrosion features observed on retrieved components.

Due to the restrictions associated with in vitro testing, it is difficult to analyse the effects of variations such as implant positioning, patient factors and surgical factors on the fretting corrosion process. Finite element (FE) simulations are more flexible to study the effect of such variations on the taper mechanics in modular THA systems.<sup>13–18</sup> Parameters such as head size,<sup>13,14,18</sup> assembly force<sup>15,16,18</sup> and taper size<sup>15,17</sup> have been varied to investigate their effect on the mechanical response of the taper junction. These FE studies have demonstrated that material combination and coefficient of friction have a significant effect on interface micro-motions (MMs) and contact pressures (CPs).<sup>15</sup> Most FE studies use input parameters based on values found in the literature.<sup>19</sup> However, the reported coefficient of friction can range from 0.15 to 0.8 for titanium-on-titanium or titanium-on-cobalt chrome material pairs.<sup>20–22</sup> Moreover, plastic deformation can occur during assembly of the taper junction, which also depends on the specific properties of the implant material. The second objective of this study was therefore to develop an FE model that was consistent with the novel fretting experiments. The FE model was then to apply loads from different activities of daily living in order to study the taper mechanics in silico rather than during simplified experimental loading conditions.

## Methods

The contact mechanics of the taper junction were investigated by adopting a combined experimental and computational approach. First, tensile assembly and disassembly experiments were performed in order to quantify taper engagement mechanics. Subsequently, experiments were performed where the taper junction was subjected to dynamic loading, to simulate the fretting patterns seen in clinical retrievals.

Both experiments, tensile (dis)assembly and dynamic loading, were replicated in FE models to validate the

computational contact mechanics and wear predictions. Subsequently, these FE models were subjected to loads occurring during activities of daily living, to analyse the effects of activity type on the fretting wear potential of the taper junction.

### *Experimental testing: tensile assembly and disassembly experiments*

Biomet Type 1 femoral stems were combined with Biomet M2a-Magnum + 9-mm offset taper adaptors. Both sets of components were manufactured from Ti6Al4V alloy. The taper adaptors were axially aligned and assembled to a 4- or 15-kN load at a crosshead speed of 1 mm/min. The test was repeated five times ( $n = 5$ ) for the 4-kN case and four times ( $n = 4$ ) for the 15-kN assembly case. The components were then disassembled in accordance with ISO 7206-10:2003 at a crosshead speed of 0.48 mm/min. The assembly and disassembly forces were applied parallel through the taper axis.

### *Experimental testing: accelerated fretting experiments*

An accelerated fretting test was developed that consistently simulated fretting wear patterns observed in some clinical retrievals. Each stem was potted using DuroCit-3 mounting material (polymethyl methacrylate (PMMA)), representing the use of bone cement in vivo, into a fully polymeric fixture, to avoid any potential galvanic effects at an angle of 10° in the coronal plane and 9° in the sagittal plane (in accordance with ISO 7206-6:2013). Hydroxyapatite powder, approximately 10 mg, with a particle size of between 60 and 75 μm, was applied using a pipette onto the dry taper surface to simulate intra-operative contamination of the taper. The adaptor was then carefully assembled onto the taper to ensure the hydroxyapatite powder was trapped between the interfaces. The engagement procedure for the adaptor was to statically load the components axially to the taper with 2, 4 or 15 kN at a rate of 50 mm/min. Three femoral stems and taper adaptors ( $n = 3$ ) were tested for each assembly condition. The test setup is shown in Figure 1 without the test medium. A rocking mobile bearing fixture was used in order to produce a toggling effect. The bearing was also laterally offset in order to provide an element of torsion. Each stem was then submerged in the test medium containing phosphate-buffered saline (PBS) and a concentration of NaCl = 90 g/L, in tap water, adjusted to pH 3.0 with HCl. This test medium was maintained at 37 °C and circulated throughout the test.

A linear motor powered material test machine (either Bose 3510 with a calibrated 7.5-kN load cell or Dartec HC10 test frame with a calibrated 10-kN load cell) was used for the accelerated fretting test. The samples were preloaded with 200 N to locate the bearing

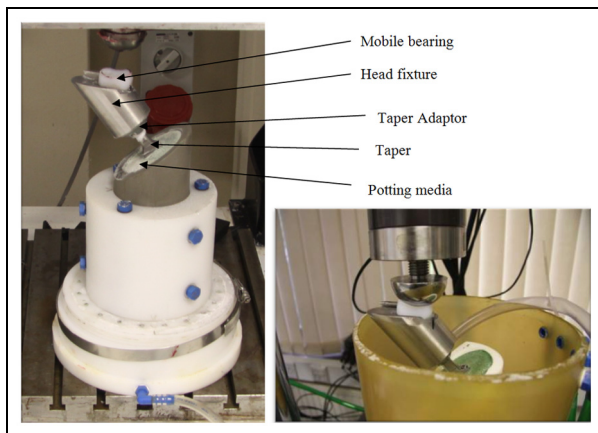


**Figure 1.** Photographs of the accelerated fretting test setup, shown without the test medium.

and ensure proper alignment of the test setup. The test was then run between 0.4 and 4 kN in a sinusoidal pattern at a frequency of 5 Hz for 10 million cycles. The 4-kN load in combination with the offset resulted in a torque of 24.8 N m and an additional bending moment of 74.2 N m about the taper.

After the accelerated fretting tests, the taper and adaptor wear was measured using a roundness measurement machine (Talyrond 585; Taylor Hobson, UK). All measurements and alignment routines were carried out using a 5- $\mu$ m diamond tip stylus at a measurement speed of 1 mm/s. Each measurement collected a series of 180 vertical traces around either the external surface of the stem taper or the internal surface of the taper adaptor. These traces were then used to map and calculate the wear in terms of volume loss from the tested components.

**FE model.** An FE model was created using geometry files from the manufacturer (Zimmer Biomet, UK) for the components tested using the accelerated fretting test detailed previously. The model was built in Abaqus 6.13 (3DS Dassault Systèmes Simulia Corp.). The femoral stem and taper adaptor were finely meshed using an element edge length of 0.2 mm at the taper interface and a more coarse mesh towards the other regions for an optimal mesh size to computational time ratio. A similar mesh size was found to be optimal in wear modelling by English et al.<sup>23</sup> A total of 158,000 elements were used for the femoral stem and taper adaptor.

The femoral stem and taper adaptor were assigned material properties derived from tensile tests using the same implant material (Ti6Al4V). Based on these tests, Young's modulus of 107 GPa and a yield stress of 865 MPa were assigned in an elastic-plastic isotropic material model.

Frictional contact at the taper junction was modelled using an isotropic penalty formulated friction coefficient. A coefficient of friction of 0.29 was applied,

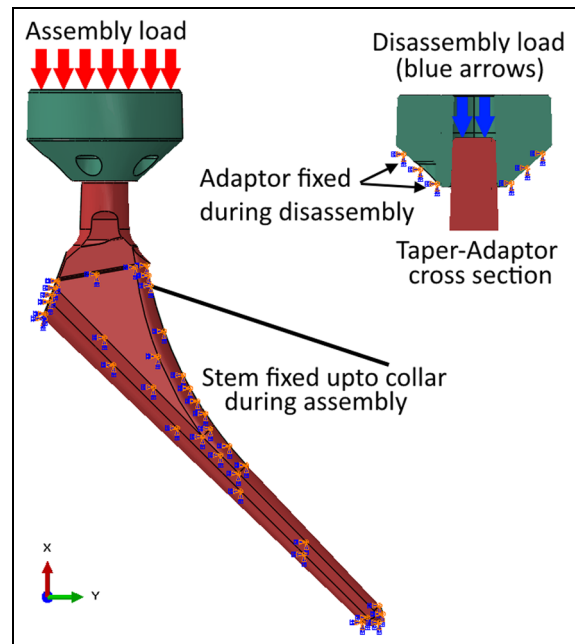


**Figure 2.** Push-on and pull-off boundary conditions.

which was determined previously in experiments using the same components.<sup>19</sup> The steps performed in the simulation were similar to the steps performed in the experimental tests.

**Simulation of the push-on and pull-off test.** To simulate the push-on and pull-off experiment, the stem was fixed up to the collar, where it would be potted in accordance with ISO 7206-6:2013. Next, the adaptor was pushed onto the taper under a load of 4 or 15 kN, parallel to the taper axis. In the subsequent step, the stem was held still, and all forces were removed in order to let the assembly relax. After relaxation, the bottom surface of the adaptor was fixed, the stem was released and pushed out of the adaptor using an increasing force, parallel to the taper axis. The maximum force was used as a quantification of the maximum pull-off force. The boundary conditions in the different steps can be seen in Figure 2.

**FE simulation of accelerated fretting.** Similar to the previous simulations, the adaptor was first assembled on the stem at a load of 2, 4 or 15 kN. After relaxation, the experimental load of 0.4 and 4 kN was replicated at the same location and under the same coronal and sagittal angles as the test setup, while fixing the stem in 6 degrees of freedom.

At the end of the simulation, the CP and MM were quantified at the nodes at the taper-adaptor interface. The MMs were quantified as the motion of a node with respect to the contacting surface between each load step. In addition, a CP and a summed MM score were calculated by performing a contact area-weighted sum of the nodal CP and MM.

To quantify taper junction wear, a wear score (WS) was defined based on Archard's law. In Archard's equation, the wear ( $W$ ) is expressed as  $W = (K \cdot F \cdot L) / H$ , where  $K$  is a wear constant that needs to be determined experimentally,  $H$  is the material hardness,  $F$  is the normal load and  $L$  is the sliding distance. For this study, the wear factor  $K$  and material hardness  $H$  were omitted, leaving a simplified version of Archard's equation that we used as  $WS = CP \cdot MM \cdot CNA$ , in which  $CP$  multiplied by the contact nodal area ( $CNA$ ) represented the normal force, and the  $MM$  defined the sliding distance. The  $WS$  was calculated for each node, after which a nodal sum of all contact nodes was performed to quantify the  $WS$  of the whole interface.

**Simulation of activities of daily living.** Finally, to investigate the effect of different activities of daily living on the  $MM$  and  $WS$ , the FE model was subjected to forces occurring in an average hip patient during normal walking, standing up from a chair and walking upstairs as reported by Bergmann.<sup>24</sup> In addition, hip joint forces during a stumbling incident of one specific patient<sup>24</sup> were applied to the FE model, as an example of an incidental peak load.

For each activity, the loading curves were split into 32 discrete steps, allowing for a quasi-static simulation. The incremental loads were applied at the centre of the head using the three-dimensional (3D) force components.<sup>24</sup> During simulation of the activities, the incremental  $MM$ s were calculated for each incremental step. These incremental  $MM$ s were then integrated over all steps to obtain the overall  $MM$  occurring at the taper surface for a specific activity. The effect of activity was analysed at an assembly load of 2 and 15 kN.

## Results

### Push-on and pull-off

Experimentally, after an assembly load of 4 kN, we found an average pull-off force of  $2.80 \pm 0.19$  kN. The FE pull-off force for the 4-kN assembly was 2.86 kN, within the range of the experimental results. The 15-kN assembly condition had an average pull-off force of  $13.76 \pm 0.40$  kN. The FE predicted a pull-off force of 11.16 kN, which was slightly lower than the experimental result.

### Accelerated fretting experiments

The experimental accelerated fretting protocol resulted in the generation of fretting marks on the taper similar to those observed on clinical retrievals (Figure 3). The volumetric wear decreased when the assembly force was increased from 2 to 4 kN or 15 kN. The lowest amount of wear was measured in the group of implants assembled at 4 kN (Figure 4). Due to the large standard



**Figure 3.** Experimental wear pattern on inferior side of the stem.

deviations, no significant difference was found between the three assembly loads.

### Simulations of accelerated fretting

In the simulations of accelerated fretting, the summed  $MM$  (Figure 5) and maximum  $CP$ s decreased with increasing assembly load (1202–930 MPa), although directly after assembly the highest peak pressure was seen in the 15-kN assembly load model (321 vs 42 MPa).

At a higher assembly load, a larger surface area was in contact ( $320 \text{ mm}^2$  at 2 kN,  $367 \text{ mm}^2$  at 4 kN and  $439 \text{ mm}^2$  at 15 kN), resulting in reduced maximum values for  $CP$  and  $MM$  (Figure 6). The larger contact surface area caused a total  $WS$  that was higher when assembled with 15 kN, which was conflicting with the experimental findings (Figure 4).

The simulated  $MM$  patterns were similar to the 'thumbprint' wear patches seen in the experimental specimens (Figure 6), with higher simulated  $MM$  and experimental wear compared to the 15-kN assembly. In the 2-kN assembly, a wear patch was observed proximally on the superior side of the taper that coincided with larger  $MM$ s in the FE plot. When assembled with 15 kN, the  $MM$  pattern moved more distally and became larger, similar to the wear patch measured in the experiments.

### Effect of activity

During the incremental loading of the simulated activities of daily living, the maximum  $CP$  was directly

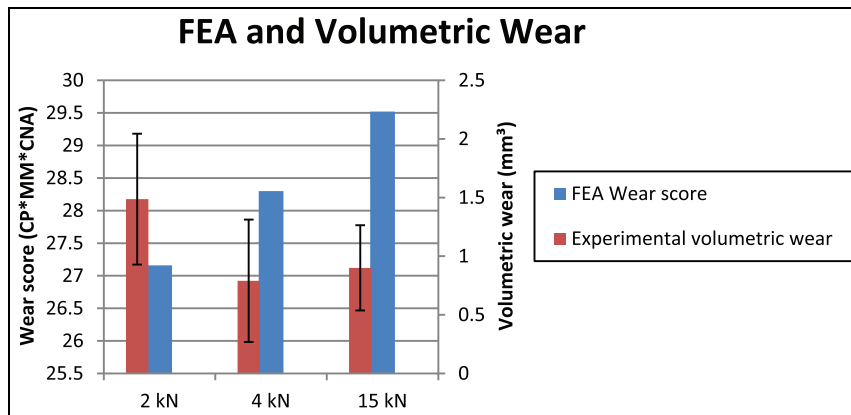


Figure 4. FE wear score and experimental volumetric wear.

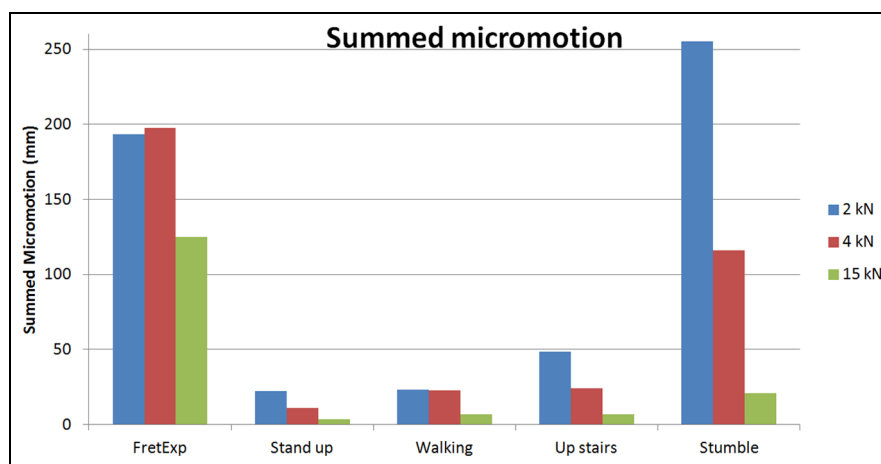


Figure 5. Summed micromotion for all activities.

related to the force increments applied to the system. However, a large variation in maximum CP was seen with an assembly load of 2 kN, particularly during the stumble load (44–313 MPa for 2 kN; 245–313 MPa for 15-kN assemblies).

The variations in the loads occurring during the activities also led to larger changes in MM between load increments, defined as incremental MM (Figure 7). In general, a higher assembly load resulted in lower incremental MM. Overall, a decrease in total summed MM was found by increasing the assembly force from 2 to 15 kN (Figure 5).

At a 2-kN assembly force, the effect of activity in MM patterns was also more pronounced (Figure 8). It is interesting to note that the maximum MM patch for normal walking appeared on the superior side of the taper (particularly for the 2-kN assembly force), whereas for all other activities, at higher assembly loads, the maximum MM patch was seen on the inferior side. Larger MMs were typically found during walking upstairs and stumbling, while normal walking and rising from a chair produced similar patterns. At an assembly load of 15 kN, the variation in activity did

not have a dramatic effect on the MM, except during the stumble load.

## Discussion

In this study, we aimed to develop an experimental setup capable of creating wear patterns found on retrieved implants and to use the outputs of this test to develop and validate an FE modelling approach that was able to analyse the effects of variants such as implant positioning, patient factors and surgical factors. In order to ensure analysis accuracy, experiments were performed to obtain consistent material properties, and tests were performed to determine the accurate coefficient of friction.<sup>19</sup>

Wear marks on the inferior side of the taper, as seen in Figure 3, show a similar pattern as seen in retrievals from several implant systems. The typical 'thumbprint'-shaped wear pattern was previously described by Langton et al.,<sup>3</sup> who suggested a toggling effect as the underlying cause. Similar patterns have been observed by Cook et al.<sup>25</sup> in both visual inspection and RedLux height maps of the taper surface. In a retrieval study,

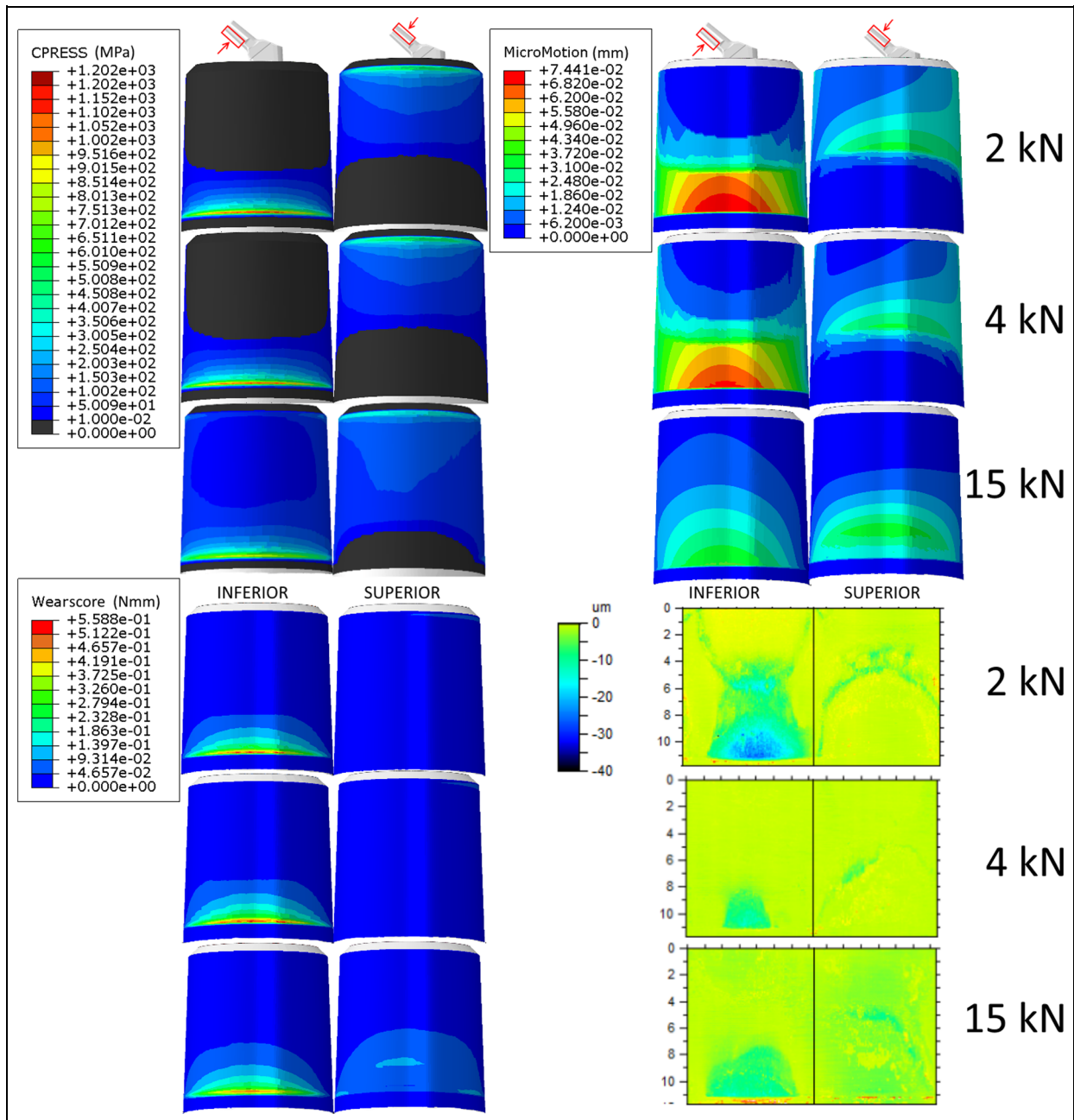


**Figure 6.** Accelerated fretting FE taper plots and linear wear Talyrd measurement plots (bottom right) for 2-, 4- and 15-kN assembly loads. The inferior views represent the ‘bottom’ side of the taper opposite of the load direction, whereas the superior views show the ‘top’ of the taper in the direction of the load.

Bishop et al.<sup>26</sup> also found tapers with thumbprint-like wear patches, in addition to specimens with an axisymmetric wear pattern.

In this study, we first tried to validate our modelling approach against the taper engagement mechanics at assembly loads of 2 and 15 kN. The FE simulations compared well to the experimental results. We then compared the predicted WSs against the volumetric wear on tapers after 10 million loading cycles for 2-, 4- and 15-kN assembled stem-adaptor combinations. In these simulations, the predicted WSs showed a trend that was opposite to the wear volumes seen experimentally. However, the computed MM distributions were

very similar to the wear patches seen in the experiments.

A possible cause for the discrepancy between the computational and experimental wear predictions may be related to the fact that the FE simulations do not account for the effect of the wear process on the changes in CP and MM. While the current simulations predict wear based on the initial contact mechanics, changes in CP and MM may alter the distribution and total volume of wear.

Another limitation of the FE simulations may be that the relationship between the wear volume, CP and MM was assumed to be linear, in accordance with

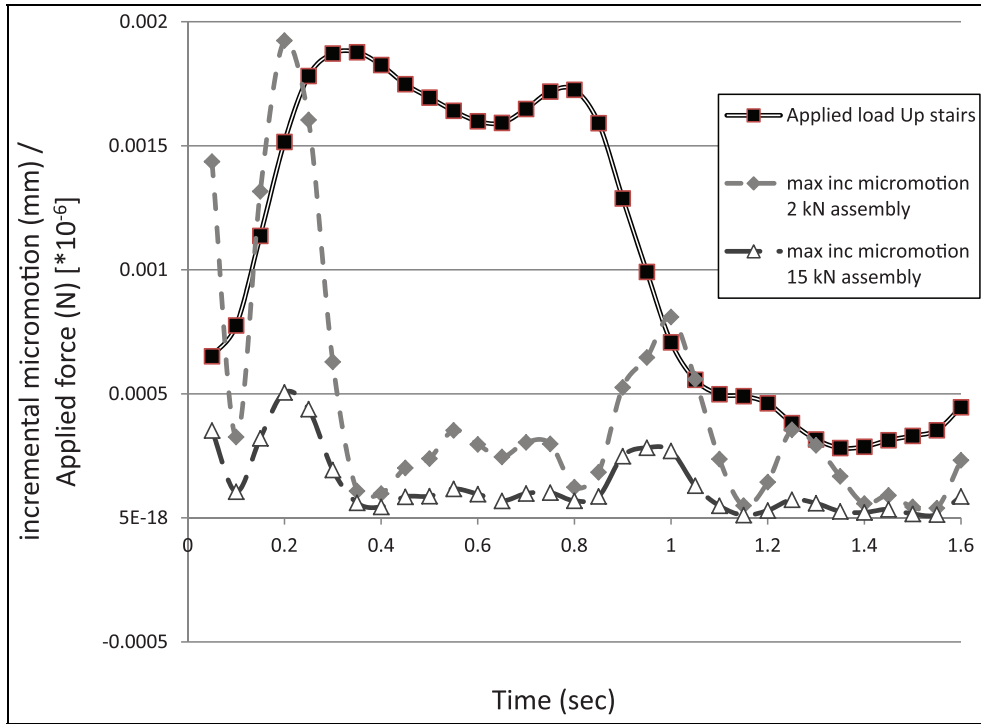


Figure 7. Incremental micromotion and load over time for 'upstairs' assembled with 2 and 15 kN.

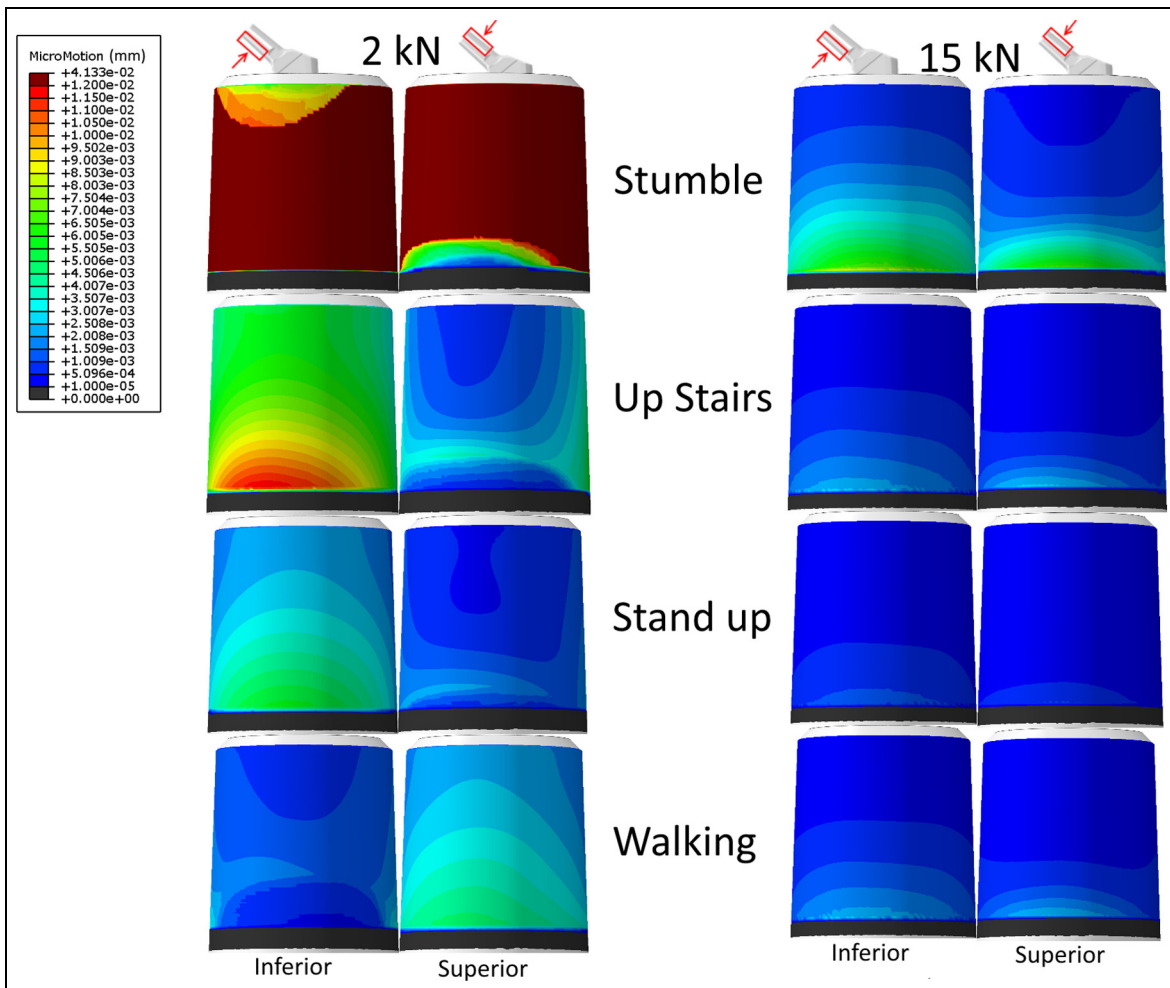


Figure 8. Micromotion plots for all activities assembled with 2 and 15 kN: inferior and superior view.

Archard's law. The fact that the predicted MM distribution was very similar to the wear patches seen on the experimental specimens may suggest that the wear may be more dependent on the MM than the CP. Archard's law might therefore not be appropriate for modelling wear at the taper junction. In other studies, wear models incorporating the shear stress instead of the CP are used.<sup>23</sup> Swaminathan and Gilbert<sup>9</sup> developed an electrochemical model of fretting wear, based on motion and contact force, which may be more appropriate for the simulation of taper fretting. At this point, it cannot be concluded that these wear models are favourable over Archard's law due to the lack of wear modelling that assesses the effect of geometry changes on the CP and MM. Another factor that has not been taken into consideration in this FE simulation is the effect of the chemical environment; the fretting test setup used a corrosive environment in order to accelerate the fretting processes; however, this has not been considered in these simulations and only the mechanical environment has been examined.

Although there was no correlation between the predicted FE WS and the measured volumetric wear, the model was used to study the taper mechanics using loading conditions of several activities of daily living. The WS results may not give a validated wear result, but the differences between the different loading conditions can give important insights in the taper mechanics.

Analyses of different activities at different assembly loads revealed that the type of activity can have a distinct effect on CP and MM at the taper junction, particularly at lower assembly loads. This further stresses the importance of assembly technique; this was also previously shown by Mroczkowski et al.,<sup>27</sup> who showed that the assembly load is important in the initial stability of modular hip taper connections. Larger MMs were found during walking upstairs and particularly during stumbling. Evidently, the number of stumbling instances is much lower than the number of cycles of the other activities, but it emphasizes the significant effect of elevated external loads on the taper mechanics.

Limitations to our experimental approach include the assembly of the components, which was performed using a statically applied load, while during surgery, the head or adaptor is assembled using impaction. While our approach may be less representative of the clinical situation, the static load was chosen to ensure consistency in the component assembly, which was shown to have a distinct effect on the experimental results. In addition, the volumetric wear was not measured incrementally throughout the test, only at the end, meaning that the wear could not be tracked with the simulations. Moreover, the number of experiments was limited to  $n = 3$ , which resulted in an insufficient statistical power to find significant differences between the different assembly groups.

Similar to Dyrkacz et al.<sup>15</sup> and English et al.,<sup>28</sup> we found that an increase in assembly force resulted in lower MM. English et al. also showed that an increase in

assembly force increases the initial CP, but over time, the increased assembly force causes a lower CP on the taper. Similar to this study, Elkins et al.<sup>18</sup> showed that increased assembly forces increase the CP and decrease the MM. Because the wear is related to both the CP and MM, Elkins et al. found that the combination of increased CP with decreased MM had a negligible effect on the wear at the taper junction interface. They found that the wear was less affected by CP or MM alone, whereas we found that the wear seems to be more driven by MM.

We showed using our experiments that an increased assembly force reduces the fretting wear at the taper interface. This highlights the clinical significance of the assembly procedure of modular components at the time of surgery. As we have shown in this work, current FE studies using Archard's law in combination with FE models which do not allow geometry updates to account for material loss cannot be validated, and their results in terms of fretting potential may be inaccurate.

In future studies, we aim to incorporate the actual wear process in our simulations, in order to account for the effect of geometrical changes at the interface on the contact mechanics. The results of the accelerated fretting tests presented in this study will serve as an input to further optimize our modelling approach.

#### Declaration of conflicting interests

The author(s) declared the following potential conflicts of interest with respect to the research, authorship, and/or publication of this article: I.K., T.M. and E.L. are employees of Zimmer Biomet and contributed to the writing of this work.

#### Funding

The author(s) disclosed receipt of the following financial support for the research, authorship, and/or publication of this article: This study was supported by Zimmer Biomet UK, Ltd.

#### References

1. McKellop HA, Sarmiento A, Brien W, et al. Interface corrosion of a modular head total hip prosthesis. *J Arthroplasty* 1992; 7: 291–294.
2. Bobyn JD, Tanzer M, Krygier JJ, et al. Concerns with modularity in total hip arthroplasty. *Clin Orthop Relat Res* 1994; 298: 27–36.
3. Langton DJ, Sidaginamale R, Lord JK, et al. Taper junction failure in large-diameter metal-on-metal bearings. *Bone Joint Res* 2012; 1: 56–63.
4. Lavigne M, Belzile EL, Roy A, et al. Comparison of whole-blood metal ion levels in four types of metal-on-metal large-diameter femoral head total hip arthroplasty: the potential influence of the adapter sleeve. *J Bone Joint Surg Am* 2011; 93(Suppl. 2): 128–136.
5. Delaunay C, Petit I, Learmonth ID, et al. Metal-on-metal bearings total hip arthroplasty: the cobalt and chromium ions release concern. *Orthop Traumatol Surg Res* 2010; 96: 894–904.



6. Swann RP, Webb JE, Cass JR, et al. Catastrophic head-neck dissociation of a modular cementless femoral component. *J Bone Joint Surg* 2015; 5: 1–5.
7. Panagiotidou A, Meswania J, Osman K, et al. The effect of frictional torque and bending moment on corrosion at the taper interface: an in vitro study. *Bone Joint J* 2015; 97-B: 463–472.
8. Goldberg JR and Gilbert JL. In vitro corrosion testing of modular hip tapers. *J Biomed Mater Res B Appl Biomater* 2003; 64: 78–93.
9. Swaminathan V and Gilbert JL. Fretting corrosion of CoCrMo and Ti6Al4V interfaces. *Biomaterials* 2012; 33: 5487–5503.
10. Geringer J, Forest B and Combrade P. Fretting-corrosion of materials used as orthopaedic implants. *Wear* 2005; 259: 943–951.
11. Duisabeau L, Combrade P and Forest B. Environmental effect on fretting of metallic materials for orthopaedic implants. *Wear* 2004; 256: 805–816.
12. Hallab NJ, Messina C, Skipor A, et al. Differences in the fretting corrosion of metal-metal and ceramic-metal modular junctions of total hip replacements. *J Orthop Res* 2004; 22: 250–259.
13. Lavernia CJ, Iacobelli DA, Villa JM, et al. Trunnion-head stresses in THA: are big heads trouble? *J Arthroplasty* 2015; 30: 1085–1088.
14. Theodorou EG, Provatidis CG, Babis GC, et al. Large diameter femoral heads impose significant alterations on the strains developed on femoral component and bone: a finite element analysis. *Open Orthop J* 2011; 5: 229–238.
15. Dyrkacz RMR, Brandt JM, Morrison J, et al. Finite element analysis of the head-neck taper interface of modular hip prostheses. *Tribol Int* 2015; 91: 206–213.
16. Fallahnezhad K, Farhoudi H, Oskouei RH, et al. Influence of geometry and materials on the axial and torsional strength of the head-neck taper junction in modular hip replacements: a finite element study. *J Mech Behav Biomed Mater* 2016; 60: 118–126.
17. Donaldson FE, Coburn JC and Siegel KL. Total hip arthroplasty head-neck contact mechanics: a stochastic investigation of key parameters. *J Biomech* 2014; 47: 1634–1641.
18. Elkins JM, Callaghan JJ and Brown TD. Stability and trunnion wear potential in large-diameter metal-on-metal total hips: a finite element analysis. *Clin Orthop Relat Res* 2014; 472: 529–542.
19. Bitter T, Khan I, Marriott T, et al. Experimental measurement of the coefficient of friction at the Ti-Ti taper connection in total hip arthroplasty. *J Biomech Eng* 2016; 138: 4032446.
20. Fessler H and Fricker DC. Friction in femoral prosthesis and photoelastic model cone taper joints. *Proc IMechE, Part H: J Engineering in Medicine* 1989; 203: 1–14.
21. Mary C and Fouvry S. Numerical prediction of fretting contact durability using energy wear approach: optimisation of finite-element model. *Wear* 2007; 263: 444–450.
22. Shareef N and Levine D. Effect of manufacturing tolerances on the micromotion at the Morse taper interface in modular hip implants using the finite element technique. *Biomaterials* 1996; 17: 623–630.
23. English R, Ashkanfar A and Rothwell G. A computational approach to fretting wear prediction at the head-stem taper junction of total hip replacements. *Wear* 2015; 338–339: 210–220.
24. Bergmann G. *HIP98 – loading of the hip joint*. 2002, <https://orthoload.com/>
25. Cook RB, Bolland BJ, Wharton JA, et al. Pseudotumour formation due to tribocorrosion at the taper interface of large diameter metal on polymer modular total hip replacements. *J. Arthroplasty* 2013; 28: 1430–1436.
26. Bishop NE, Witt F, Pourzal R, et al. Wear patterns of taper connections in retrieved large diameter metal-on-metal bearings. *J Orthop Res* 2013; 31: 1116–1122.
27. Mroczkowski ML, Hertzler JS, Humphrey SM, et al. Effect of impact assembly on the fretting corrosion of modular hip tapers. *J Orthop Res* 2006; 24: 271–279.
28. English R, Ashkanfar A and Rothwell G. The effect of different assembly loads on taper junction fretting wear in total hip replacements. *Wear* 2015; 95: 199–210.